SAND2019-14226C

Sarin on Defective Metal-Organic Framework UiO-66: An Infrared Spectroscopy Study Combined with Density Functional Theory

Monica McEntee[1], Jacob Harvey[2], Sergio Garibay[3], Erin Durke[1], Jared DeCoste[1], Jeffery Greathouse[2], and Dorina Sava Gallis[2]

[1]Combat Capabilities Development Command Chemical Biological Center, Aberdeen Proving Ground, MD, [2]Sandia National Laboratories, Albuquerque, NM, [3]Leidos, Reston, VA

Abstract

Recent real-world events have emphasized the importance in developing efficient technologies for degrading organophosphorous compounds. Metal-organic frameworks (MOF) are nanoporous materials that have been studied by many in academia and the Army in the past decade because of their high surface areas, catalytic chemical warfare agent (CWA) decomposition in buffer solution,[1] and composition tunability. One MOF in particular, UiO-66, has a base unit consisting of a $Zr_6O_4(OH)_4$-octahedron secondary building unit connected via 1,4-benzene-dicarboxlate (BDC) linkers, and has been found to be highly stable in air and water.[2] For all of the advantages UiO-66 and MOFs (in general) have, the role defects in the crystal structure play in adsorption and reactivity is not well understood. Here we report a detailed transmission infrared spectroscopy (TIR) study of a CWA, Sarin (GB), and its in-situ adsorption and subsequent reactivity on defective UiO-66. We look at not just one but multiple IR modes including the P=O, C-H, C-O, P-CH_3, and P-F moieties to help understand the binding mechanism on the surface. Density functional theory calculated IR spectra confirm that multiple favorable binding sites exist within the MOF[3] and that these sites lead to characteristic shifts in the P=O stretch frequency. Understanding these mechanisms can help us design MOFs to specific threats or applications for protection and decontamination.

Experimental Setup

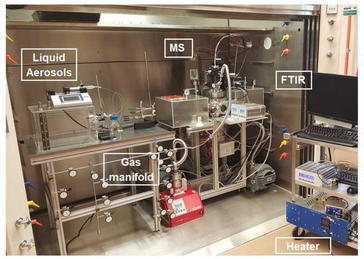

Figure 1. Picture of high-vacuum chamber setup. The techniques include transmission IR and mass spectrometry (MS).

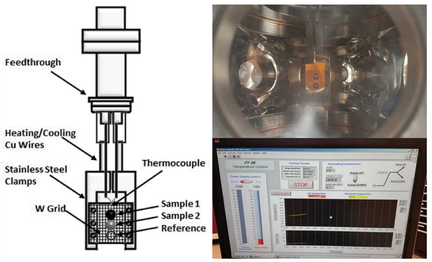

Figure 2. (Left) Schematic of sample holder and manipulator. (Right) Pictures of sample in the chamber (top) and the LAB VIEW program for temperature control of the sample.

Surface Characterization & Experimental Method

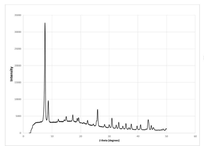

Figure 3. X-Ray Diffraction pattern of UiO-66. This pattern indicates the sample is crystalline.

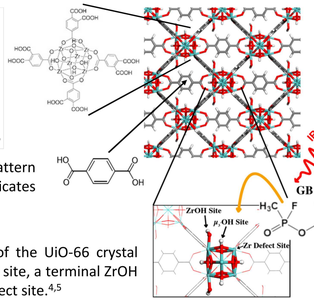

Figure 4. DFT calculation of the UiO-66 crystal structure including an ideal site, a terminal ZrOH site, a μ_3-OH site, and a defect site.[4,5]

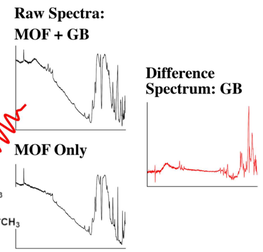

Figure 5. IR spectra of MOF + GB, MOF only, and the subtracted IR spectra.

Infrared Spectra of Sarin Adsorption on UiO-66

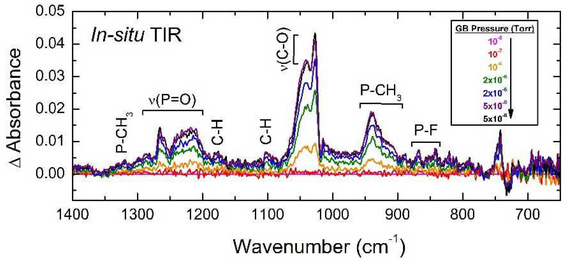

Figure 6. Difference spectra of GB exposure on UiO-66 with the MOF IR bands removed. The background for these spectra is the W-grid with the MOF present before GB exposure. This Figure shows the growth of the GB IR bands as a function of GB pressure. The pressures of GB exposure are at 10^{-8} (pink curve), 10^{-7} (red curve), 10^{-6} (orange curve), $2x10^{-6}$ (green and blue curves), and $5x10^{-6}$ (purple and black curves) Torr on UiO-66.

Sarin Binding Sites on UiO-66: Experiment and Theory Comparison

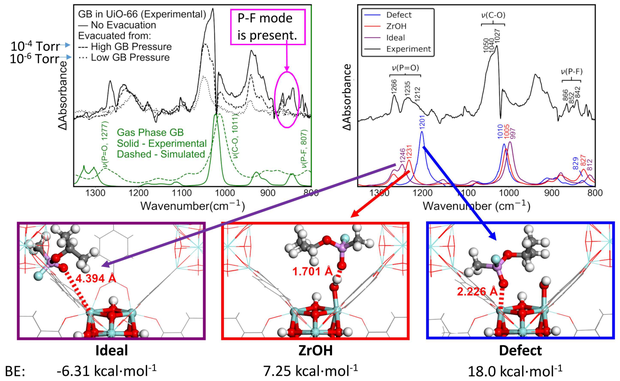

BE: -6.31 kcal·mol^{-1} 7.25 kcal·mol^{-1} 18.0 kcal·mol^{-1}

Figure 7. (Top, left) Difference spectra of GB exposure on UiO-66 at different GB concentrations. As the pressure of GB increases, the coverage of GB on the surface increases, and the P=O IR bands blueshift from one site to another as each site becomes saturated. ***The presence of the P-F mode confirms GB is adsorbed and does not decompose.***

(Top, right) The experimental IR spectrum with the most GB coverage on the UiO-66 surface is compared to different IR calculated spectra to determine the different sites on the surface and their corresponding IR bands. The most redshifted (lowest wavenumber, cm^{-1}) P=O IR band at 1212-1200 cm^{-1} corresponds to GB adsorbed on the defect site; the P=O IR band at 1235-1231 cm^{-1} corresponds to the ZrOH site; lastly, the P=O IR band at 1266-1246 cm^{-1} corresponds to the ideal Zr site. Each adsorption site is depicted in a calculated schematic in the boxes. The binding energies increase from ideal < ZrOH < defect site.

Orientation Dependent Sarin Adsorption on UiO-66

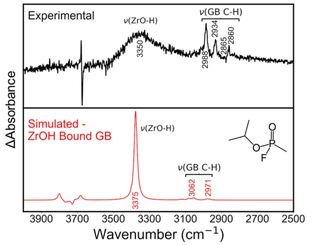

(Left) The OH region shows a blueshift in the μ_3-OH mode, which indicates no adsorption on that site; whereas, the ZrOH mode redshifts and broadens, which indicates GB adsorption on that site.

(Right) The CH region has a new IR mode at ~2860 cm^{-1}, which could represent the propoxy- or P-CH_3- group interacting with the ZrOH site.

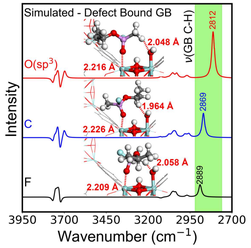

Sarin Degradation upon Heating in Vacuum

Sarin does not react on a dry UiO-66 surface in vacuum. However, upon heating from room temperature (yellow curve) up to 400K (brown curve), GB decomposes via the conversion of the P=O modes at 1257-1212 cm^{-1} to O-P-O modes at 1178 and 1090 cm^{-1}. Additionally, the loss of C-O, P-CH_3, and P-F modes and the gain of new IR bands at lower wavenumbers confirm decomposition. We cannot rule out partial GB desorption as well.

If water was present on the surface, GB decomposition would likely occur even at room temperature.

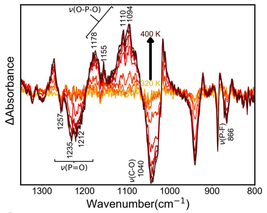

Conclusions & Future Work

GB adsorbs on UiO-66 at room temperature intact, and onto several different adsorption sites (ideal Zr site, ZrOH site, and the defect site) in increasing order of binding energy. The geometrical orientation of GB affects the CH modes in the IR spectrum to help identify the exact binding orientation. Additionally, GB decomposes on UiO-66 after heating the surface above 340K with no H_2O present. Future work includes looking at GB interactions with MOFs with water present, and with isotopically-labeled GB and H_2O to elucidate reaction mechanisms.

References

1. Mondloch *et al.* Nature materials **2015**, *14*(5), p.512.
2. DeCoste, J.B. *et al.* Journal of Materials Chemistry A **2013**, *1*(18), pp.5642-5650.
3. Harvey, J.A. *et al.* The Journal of Physical Chemistry C **2018**, *122*(47), pp.26889-26896.
4. Hod, I. *et al.* Nature communications **2015**, *6*, pp.8304.
5. Rogge, S.M. *et al.* Chemical Society Reviews **2017**, *46*(11), pp.3134-3184.

Sandia National Laboratories

Acknowledgements: We thank Bryan Schindler and Eric Bruni for assisting in chemical warfare agent handling experiments. Additionally, the authors thank Darren Driscoll and John Morris for the design and development of the vacuum system. This work is supported by the Laboratory Directed Research and Development Program at Sandia National Laboratories. Sandia National Laboratories is a multimission laboratory managed and operated by National Technology and Engineering Solutions of Sandia, LLC., a wholly owned subsidiary of Honeywell International, Inc., for the U.S. Department of Energy's National Nuclear Security Administration under contract DE-NA-0003525. The views expressed in this article do not necessarily represent the views of the U.S. Department of Energy or the United States Government. **This work has been published in *J Phys Chem Lett*, 10(17), pp 5142-5147.**